Advances in Atom and Single Molecule Machines
*Series Editor:* Christian Joachim

André Gourdon *Editor*

# On-Surface Synthesis

## Proceedings of the International Workshop On-Surface Synthesis, École des Houches, Les Houches 25–30 May 2014

Springer

# Contents

**The Emergence of Covalent On-Surface Polymerization** . . . . . 1
Christophe Nacci, Stefan Hecht and Leonhard Grill

**Transition Metals Trigger On-Surface Ullmann Coupling Reaction: Intermediate, Catalyst and Template** . . . . . 23
L. Dong, S. Wang, W. Wang, C. Chen, T. Lin, J. Adisoejoso and N. Lin

**On-Surface (Cyclo-)Dehydrogenation Reactions: Role of Surface Diffusion** . . . . . 43
José A. Martín-Gago, Anna L. Pinardi and José I. Martínez

**Enediyne Cyclization Chemistry on Surfaces Under Ultra-High Vacuum** . . . . . 85
Dimas G. de Oteyza

**On-Surface Synthesis by Azide–Alkyne Cycloaddition Reactions on Metal Surfaces** . . . . . 101
Oscar Díaz Arado, Harry Mönig and Harald Fuchs

**On-Surface Synthesis of Phthalocyanine Compounds** . . . . . 115
E. Nardi, M. Koudia, S. Kezilebieke, J.-P. Bucher and M. Abel

**Molecular On-Surface Synthesis: Metal Complexes, Organic Molecules, and Organometallic Compounds** . . . . . 131
J. Michael Gottfried

**On-Surface Synthesis of Single Conjugated Polymer Chains for Single-Molecule Devices** . . . . . 167
Yuji Okawa, Swapan K. Mandal, Marina Makarova, Elisseos Verveniotis and Masakazu Aono

**On-Surfaces Synthesis on Insulating Substrates** . . . . . 181
Markus Kittelmann, Robert Lindner and Angelika Kühnle

**Bottom-Up Fabrication of Two-Dimensional Polymers on Solid Surfaces** . . . . . 199
Markus Lackinger

**On-Surface Dynamic Covalent Chemistry** . . . . . 221
Jie-Yu Yue, Li-Jun Wan and Dong Wang

**Synthesis of Atomically Precise Graphene-Based Nanostructures: A Simulation Point of View** . . . . . 237
L. Talirz, P. Shinde, D. Passerone and C.A. Pignedoli

**Formation Mechanisms of Covalent Nanostructures from Density Functional Theory** . . . . . 269
Jonas Björk

# The Emergence of Covalent On-Surface Polymerization

**Christophe Nacci, Stefan Hecht and Leonhard Grill**

**Abstract** The covalent linking of molecular building blocks directly in the two-dimensional confinement of a surface, the so-called on-surface polymerization, has developed rapidly in the last years since it represents a reliable strategy to grow functional molecular nanostructures in a controlled fashion. Here, we review the growth of such structures via on-surface Ullmann coupling and highlight the major chemical and physical aspects. These systems are typically studied by scanning tunneling microscopy that allows exploration of the initial monomer species, intermediate products and final nanostructures with sub-molecular spatial resolution. In this way, the chemical structures of the ex situ synthesized molecular building blocks are directly correlated with the outcome of the chemical reaction. We also present examples with different monomer species in view of growing heterogeneous molecular structures as well as the importance of the molecular interaction with the template surface as a further key parameter to control the molecular diffusion and tune the final molecular architecture.

## 1 Introduction

Assembling functional molecular building blocks on a surface is a promising route toward central objectives of nanotechnology and in particular molecular electronics since it might allow the growth of electronic circuits based on the functionalities of individual molecular species [1, 2]. Other bottom-up strategies lead to the growth of

C. Nacci · L. Grill (✉)
Department of Physical Chemistry, Fritz-Haber-Institute of the Max-Planck-Society, 14195 Berlin, Germany
e-mail: leonhard.grill@uni-graz.at

C. Nacci · L. Grill
Department of Physical Chemistry, University of Graz, 8010 Graz, Austria

S. Hecht (✉)
Department of Chemistry, Humboldt-Universität zu Berlin, 12489 Berlin, Germany
e-mail: sh@chemie.hu-berlin.de



A. Gourdon (ed.), *On-Surface Synthesis*, Advances in Atom and Single Molecule Machines, DOI 10.1007/978-3-319-26600-8_1

extended surface supported two-dimensional networks with outstanding technological relevance [3, 4]. Thus, although the precursor molecules do not contain a function in these cases, the assembly of molecules in the two-dimensional confinement of a surface can be very efficient. In the field of weaker intermolecular interactions, many successful attempts of growing supramolecular patterns at surfaces [5–8] have been achieved. However, the use of covalent linking to stabilize molecular arrangements at surfaces attracted considerable attention in the last years [9–27], becoming nowadays a well-established technique. This approach results in the presence of molecular polymers on surfaces that could hardly be deposited onto the surface under clean conditions by using conventional techniques and preventing any defragmentation process [28]. The nature of the covalent bond provides high stability and robustness to the resulting nanostructures and allows for efficient "through bond" charge transport [29–31].

In this chapter, we review the development and conceptual foundation of the covalent on-surface polymerization technique. As our and many others' work is based on the Ullmann reaction [32], we focus on the aryl–aryl homocoupling of halogenated monomer building blocks typically performed on coinage metal surfaces. We first provide chemical considerations regarding the reaction mechanism and derive critical parameters for successfully carrying out on-surface polymerizations. Using this approach covalently bound molecular assemblies with a predefined shape and size are produced under ultrahigh vacuum (UHV) conditions. We show how the final topology of the desired molecular aggregates is intimately connected to the design of the single-molecule building constituents. Different growth strategies, e.g., one-step versus two-step (hierarchical) processes, can eventually lead to the same final molecular architecture: the major differences between the two cases are highlighted. The substrate surface corrugation can be furthermore exploited to drive on-surface synthesis processes along certain directions and promote the growth of nanostructures with predefined orientations. In this regard, the importance of the surface anisotropy is discussed.

## 2 Results and Discussions

### *2.1 On-Surface Polymerization Technique*

In general, the on-surface assembly of molecular building blocks into large and extended structures according to a bottom-up scheme can be achieved by different strategies. If stabilized by rather weak non-covalent intermolecular interactions [5–8, 33], these nanostructures belong to the field of supramolecular chemistry [34]. For instance dipole–dipole interactions have been used to govern the molecular aggregation of porphyrin derivatives, carrying two *trans*-positioned cyanophenyl groups, into long linear chains on a Au(111) surface (Fig. 1a) [6]. Two opposing cyanophenyl groups can engage in a self-complementary dipolar interaction (hydrogen bond) thereby driving and directing the self-assembly into elongated porphyrin chains.

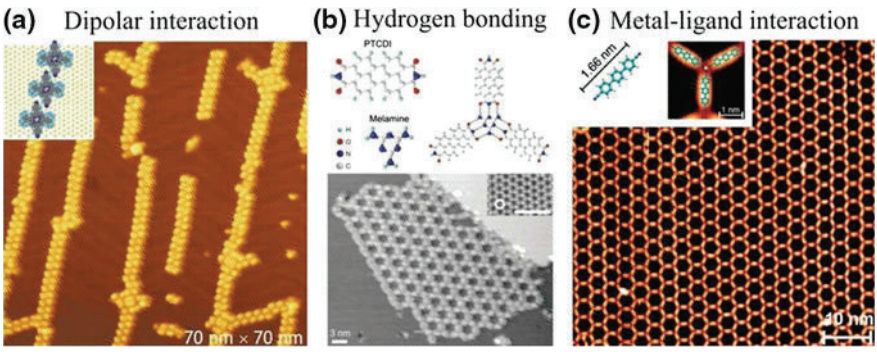


**Fig. 1** Supramolecular self-assembled molecular structures. **a** STM image at 63 K of trans-BCTBPP wires hold together via dipole–dipole interactions on Au(111) (Reproduced from [6], with permission). **b** Two-dimensional networks of PTCDI and melamine molecules stabilized via H-bonding (model structures of the molecules and network in the upper panel). In the lower panel, an STM image of the network (−2 V, 0.1 nA). In the *inset*, a high-resolution view of the Ag/Si(111)-$\sqrt{3} \times \sqrt{3}$R30° is shown (Reprinted by permission from Macmillan Publishers Ltd: Nature [7], copyright 2003). **c** STM topographic image of an extended and highly regular networks formed by Codirected assembly of NC–$Ph_3$–CN linkers. In the *inset*, the structure of the molecule including its length and STM topography of the threefold *Co*–carbonitrile coordination motif with model structure is shown (Adapted with permission from Schlickum et al. [8]. Copyright 2007 American Chemical Society)

A more conventional and stronger multiple hydrogen bonding motif was used to stabilize a two-component mixture of 3,4,9,10-perylenetetracarboxylic diimide (PTCDI) and melamine molecules into a honeycomb pattern on a metal surface (Fig. 1b) [7]. The threefold symmetrical melamine molecules represent the branch points of the hexagonal network, while the PTCDI molecules serve as straight connectors (Fig. 1b). The assembly geometry allows for the local formation of three hydrogen bonds for each complementary melamine–PTCDI connection and this rather strong non-covalent interaction plays the key role in guiding the mentioned species into largely extended supramolecular networks. Moreover, many examples of two-dimensional molecular assemblies have been reported in the field of metallo-supramolecular chemistry where metal atoms are used to bridge suitably functionalized molecular units (ligands). The metal–ligand bond is typically stronger as compared to hydrogen bonding and this allows the formation of more robust networks [33]. Such metal–ligand interactions have, for example, been exploited to fabricate two-dimensional architectures based on the coordination of rod-like dinitrile molecules (NC–$Ph_n$–CN) to cobalt centers (Fig. 1c) [8].

In addition to these interactions, the formation of even stronger covalent carbon–carbon bonds between molecules on the surface gained large attention in the last years [9–18, 30, 31, 35]. The nature of the covalent bond allows to confer high stability and durability to the molecular structures, in contrast to non-covalent intermolecular bonds-based structures. This property is a key when thinking of potential use in future applications [2]. In analogy to the approach here, the

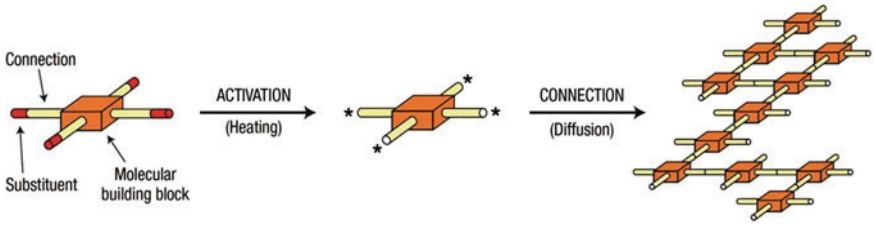


**Fig. 2** Covalently linked molecular architectures by on-surface polymerization. Single building blocks are synthesized ex situ with halogen substituents. After being thermally activated, the species diffuse across a surface, interact to each other and the formation of new carbon–carbon covalent bonds take place at the activated sites positions [9]

bottom-up growth of large networks as graphene [3] and boron nitride [4] sheets also led to highly stable structures, because of the covalent nature of their links.

The concept of the on-surface polymerization technique is illustrated in Fig. 2. Each single building block is based on a chemically stable molecular unit carrying a certain number of potentially reactive sites at specific positions. These sites are represented by a carbon–halogen bond that has a bond dissociation energy lower than all other bonds in the molecular framework. After depositing the molecules on a surface, the halogen substituents are activated (i.e., halogen–carbon bond dissociation) thermally, leaving the chemical structure of the molecular building blocks intact. At the same time, the new species thermally diffuse over the surface and form new covalent C–C bonds at the activated site positions when they get close to each other.

The design and ex situ synthesis of molecules with different numbers and arrangements of interconnection points opens up the possibility to precisely tune the topology of the final molecular architecture. Before detailing the architectural control achievable using the on-surface polymerization approach, a few aspects regarding the chemistry of both the monomers as well as the surfaces need to be considered. Due to its dominant use in the field and its importance for our own work, we limit the following discussion to the Ullmann reaction.

## 3 Chemical Considerations

When considering an Ullmann coupling reaction [32] as the connection sequence for an on-surface polymerization, several key criteria have to be met. First, one needs to design monomers, which on the one hand have to be reactive at the desired connection sites to allow for regioselective activation, for example, by carrying labile halogen substituents, yet otherwise need to be stable at the deposition and reaction conditions. In addition, the activated monomers also have to be mobile on the surface to diffuse to other monomers and the growing polymer. The latter point inevitably also depends on the surface, which needs to stabilize the formed aryl

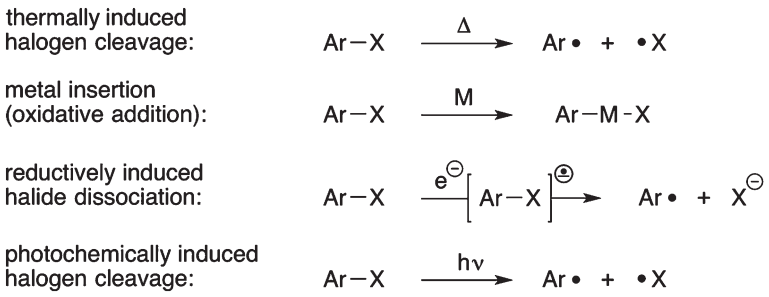


**Fig. 3** Possible activation mechanisms for aryl halides to initiate covalent on-surface polymerization

radical intermediates, yet also has to provide mobility and ideally facilitate both the activation and connection steps, i.e., act as template and catalyst.

While these aspects generally apply to most on-surface polymerization reactions, there are some specific aspects when focussing on the Ullmann reaction. The reaction can be initiated by several different dissociation mechanisms caused simply by heat (in absence or presence of a metal catalyst), electrons (from the tip of an STM, and electrode or a reducing agent) or photons (Fig. 3).

While in all cases the aryl–halogen single bond is broken, the technique/stimulus used for activation potentially provides control over where the Ullmann reaction and hence polymerization is taking place. In contrast to the pioneering work of the Rieder group on the dimerization of iodobenzene induced with the STM tip at the step edge of a Cu(111) surface [36] the majority of the reported work has been exploring thermal activation mostly in conjunction with coinage metal substrates. Hereby, the temperature required for dissociation of the halogen substituent crucially depends on the type of halogen (and potentially also on the type of (het)aryl moiety) as well as the type of substrate. The first aspect has been exploited by us for the hierarchical growth of two-dimensional polyporphyrin networks (see below), where we utilize sequential activation of first iodine and then bromine substituents to separate the two orthogonal growth directions [35]. While the C–I bonds are cleaved at 120 °C, the C–Br bonds cleave at 250 °C on the employed Au(111) surface. Of course, the latter is important as well since similar C–I bonds cleave at much higher temperatures in the absence of a coinage metal as shown by the work of Gourdon, Kühnle, and coworkers on calcite ($CaCO_3$), where temperature above 300 °C are necessary for activation [37].

Clearly and not surprisingly in the context of the classic Ullmann work using copper species [32], coinage metals facilitate activation and aryl–aryl coupling [38]. However, there are two opposing effects when comparing the coinage metals with regard to their ability to aid on-surface Ullmann type polymerization: On the one hand the higher reactivity of less noble copper surfaces aids both the initial halide dissociation as well as the coupling of the activated aryl monomers but also significantly lowers the mobility and hence diffusion of the monomers and growing

polymers, thereby inhibiting growth. Fasel and coworkers have actually engaged in a detailed comparative study showing these opposing effects for the Cu(111), Ag (111), and Au(111) surfaces [39]. The authors found the onset of network formation from hexa(*meta*-phenylene) macrocyclic hexaiodide monomers to occur at 200 °C for Cu(111), while on Au(111) 250 °C and on Ag(111) 300 °C were required. However, the morphology of the obtained poly(1,3,5-phenylene)s differs significantly as the Cu(111) grown structures are highly branched fractal-like while in the case of Ag(111) extended high-quality 2D networks were formed. Based on their experimental findings as well as theoretical investigations, they conclude that the lower activity of Ag(111) in the aryl–aryl coupling combined with the higher monomer mobility (diffusion) on this surface, both compared to Cu(111), lead to better network formation. In our work we have been mostly focussing on gold surfaces that provide a good compromise between these features. Note that even with one and the same metal its surface reconstruction plays an important role as shown by our own work (see below) as well as others [40].

In addition, defects, step edges, and adatoms are of utmost importance as they can facilitate activation (see below) [41], stabilize intermediates, and even inhibit their coupling. This is nicely illustrated by the fact that activated aryl monomers cannot be considered as truly "free radicals" but are strongly stabilized be the metal surface [39]. This also prevents skeletal rearrangements to take place and thereby assures regioselective coupling at the initially halide-substituted positions (Fig. 4).

Depending on the presence of adatoms, an alternative coupling mechanism involves the formation of an aryl–metal–aryl intermediate, which can reductively eliminate to form the desired aryl–aryl connection (Fig. 4). While this sequence has in fact successfully been observed by Lin and coworkers to take place in the polymerization of 4,4″-dibromoterphenyl on a Cu(111) surface [42], in many cases the intermediately formed copper complexes are rather stable and cannot be forced to eliminate the desired products [43, 44]. For example, using hexabenzo-coronene (HBC) dibromide monomers on Cu(111) gave Cu-bridged HBC chains; however, on a Au(111) surface the corresponding gold complexes were not observed and hence covalent aryl–aryl connections could successfully be obtained (Fig. 5)

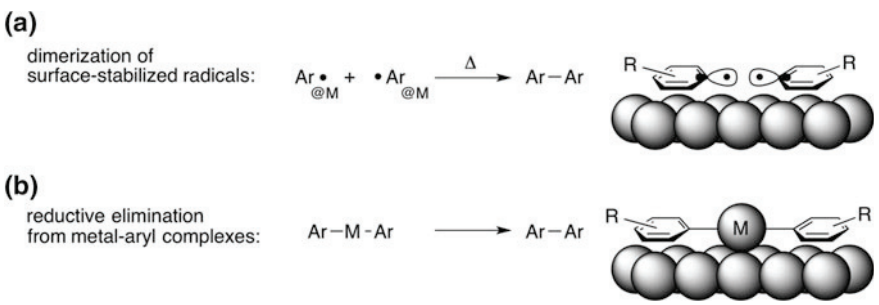


**Fig. 4** Possible coupling mechanisms for aryl halides to initiate covalent on-surface polymerization: regioselective coupling (**a**) and aryl–aryl connection via an intermediate formation of an aryl–metal–aryl intermediate (**b**)

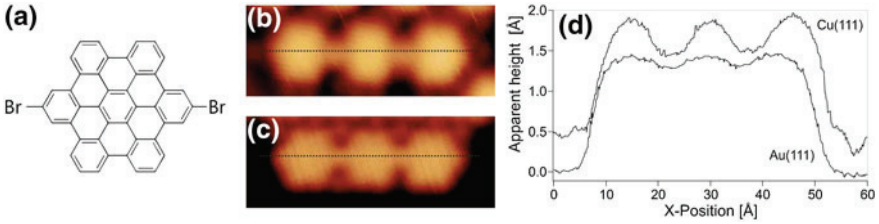


**Fig. 5** **a** Chemical structure of $Br_2$–HBC. **b** Cu-bridged HBC chain on Cu(111) (5.5 × 2.0 $nm^2$, −300 mV, 0.3 nA). **c** HBC chain on Au(111) (5.5 × 2.0 $nm^2$, −300 mV, 0.1 nA). **d** Height profiles in STM images along a HBC trimer on Cu(111) and Au(111) [43]

[43]. Therefore, not only the type of surface but also the availability of adatoms seems to have a marked effect on the polymerization outcome.

In general, we note that using the Ullmann reaction poses two inherent limitations to the on-surface polymerization process. First and foremost, the reaction is irreversible under the employed conditions, i.e., formed defects cannot be healed. Therefore, the outcome of the reaction solely relies on kinetic control and equilibration to the global thermodynamic minimum structures cannot be used as often the case for non-covalent self-assembly or dynamic covalent chemistry [45]. Using other connections such as boronic esters or imines this drawback can be overcome, however, at the cost of stability (toward hydrolysis) and functionality (in an optoelectronic context). Second, the employed polymerization approach is that of a step growth, more precisely a polycondensation, and therefore intrinsic limitation with regard to polymerization efficiency and control over the polymerization outcome exist. After sketching the chemical basis for making aryl–aryl connections, we will now detail the method of covalent on-surface polymerization and highlight the means of controlling the formed polymer structures.

## 4 On-Surface Synthesis of Covalently Bound Nanostructures

Two alternative methods can be used for the activation of molecular building blocks (methods I and II) and the growth of covalently bound nanoarchitectures, leading to similar results [9]. In method I, intact molecules are first deposited onto a surface and subsequently thermally activated. Conversely, in method II, the activation of molecular species takes place already into the evaporator cell and they are deposited onto the surface.

In both cases, the covalent linking takes place on the supporting surface upon thermal diffusion. As a first candidate for on-surface synthesis, a porphyrin building block with four bromine substituents ($Br_4$TPP) has been used (inset of Fig. 6a). If the evaporator temperature was 550 K or lower during deposition, large and ordered islands of intact $Br_4$TPP were found as a result of molecular diffusion at the surface

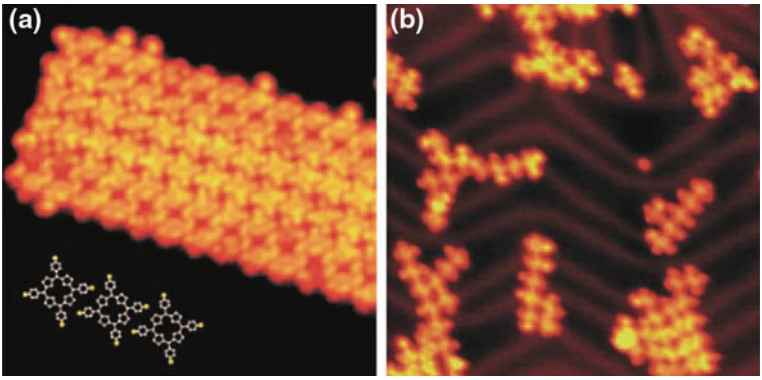


**Fig. 6** Molecular nanostructures formed by different approaches (methods I and II). **a** STM image (20 × 20 $nm^2$) of a $Br_4TPP$ molecular island on Au(111) after deposition at low evaporator temperature of 550 K onto the substrate surface kept at room temperature. Molecules are deposited intact onto the surface. The *inset* shows the chemical structure of $Br_4TPP$. **b** STM image (41 nm × 41 $nm^2$) for deposition at elevated evaporator temperature of 610 K. This causes the activation of the molecular species into the evaporator and subsequently the formation of covalently bound structures onto the surface. The Au(111) sample was cleaned by repeated Ne ion sputtering ($E$ = 1.5 keV) and subsequent annealing up to 720 K. Measurements were performed under UHV conditions with a low-temperature STM operated at a temperature of 10 K. STM images were recorded in constant current mode with the bias voltage referring to the sample with respect to the STM tip [9]

(method I, Fig. 6a). A careful analysis of the outer border of the molecular island reveals that many molecules have only three Br atoms connected while there are four on the intact molecules. This suggests that the used evaporator temperature is enough to initiate the Br dissociation of a small amount of molecules (more than 90 % of the molecules remain intact).

At higher evaporator temperatures (Fig. 6b) most of the molecules are activated with the loss of several Br substituents in the evaporator (method II). The activated species can react with each other on the surface and form new intermolecular bonds upon thermal diffusion, leading to the formation of covalently bound structures with different sizes and shapes (Fig. 6b).

To investigate the ability to control the architecture of the final molecular nanostructures, different TPP-based monomer building blocks have been synthesized with one, two, and four Br substituents (Fig. 7a–c). Intact molecules have been identified by using low evaporator temperatures: the STM images after the preparation show clearly the expected different structures (Fig. 7d–f). All species have been deposited onto a Au(111) surface kept at low temperature (to suppress any carbon–halogen bond dissociation) and afterwards annealed to thermally activate the Br dissociation. Thus, the topology of the molecular architectures is intrinsically encoded in the design of the single monomer building block (cf. first and third rows of Fig. 7).

If the monomer building block provides just one reactive side (BrTPP, Fig. 7a), the only possible result is a dimer. Porphyrin building blocks carrying two reactive sides

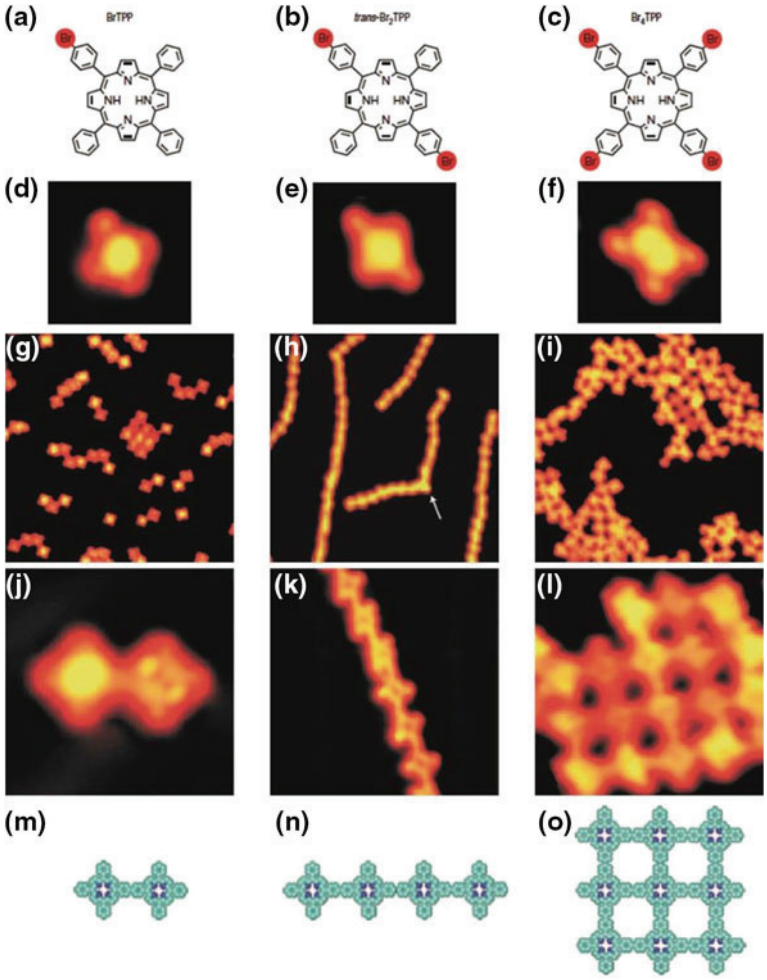


**Fig. 7** Building nanoarchitectures using different monomer building blocks carrying one (*left column*, prepared by method I), two (*middle column*, prepared by method II) and four (*right column*, prepared by method I) Br substituents (**a–c**). STM images (3.5 × 3.5 $nm^2$) of the single intact molecules (**d–f**). Overview STM images (30 × 30 $nm^2$) of the nanostructures after activation and connection (**g–i**). Detailed STM images of the resulting nanoarchitectures (**j** 5 × 5 $nm^2$; **k** 10 × 10 $nm^2$; **l** 8.5 × 8.5 $nm^2$). Corresponding chemical structures of the nanostructures (**m–o**). Measurements were performed under ultrahigh vacuum (UHV) conditions with a low-temperature scanning tunneling microscope (STM) operated at a temperature of 10 K. Covalently linked molecular structures were produced in case of method I from molecular building blocks via on-surface polymerization [9], i.e., dehalogenation at a typical temperature of 523 K (bromine dissociation) for 10 min and subsequent covalent linking of the molecules [9]

as trans-$Br_2$TPP (Fig. 7b) allows accordingly the formation of long and linear chains as shown in Fig. 7h, k. When all four porphyrin unit legs carry Br substituents (Fig. 7c), the construction of two-dimensional molecular network is enabled (Fig. 7i, l). This proves that a careful choice of the molecular design, i.e., the arrangement of the active end groups within the molecular framework of the single building block, and a successful ex situ organic synthesis of the initial building blocks give high control over the final architecture of the molecular structures.

An important issue is the precise chemical nature of the newly formed intermolecular bonds (or intramolecular bonds in the final polymer, respectively). The first evidence comes from the distances between the building blocks, which is characteristic for such a bond. There is a good agreement between the experimentally measured neighboring porphyrin cores interdistance (17.2 ± 0.3 Å) and the DFT-calculated distance (17.1 Å) calculated for a covalently bound porphyrins dimer (Fig. 8d). Furthermore, the covalent nature of the intermolecular bonds can be investigated by STM single-molecule manipulation. Molecular islands made of intact $Br_4$TPP (Fig. 6a) are easily disassembled by STM-based lateral manipulation [9]. In contrast, dimers, chains, and molecular networks (Fig. 7) can follow the STM tip pathway during a pulling experiment [30, 31] without undergoing fragmentation processes. This is a clear signature for the robustness of the intermolecular bonds within the molecular structures after the end-group legs activation. Consequently, the interpretation as a covalent bond seems reasonable. Other

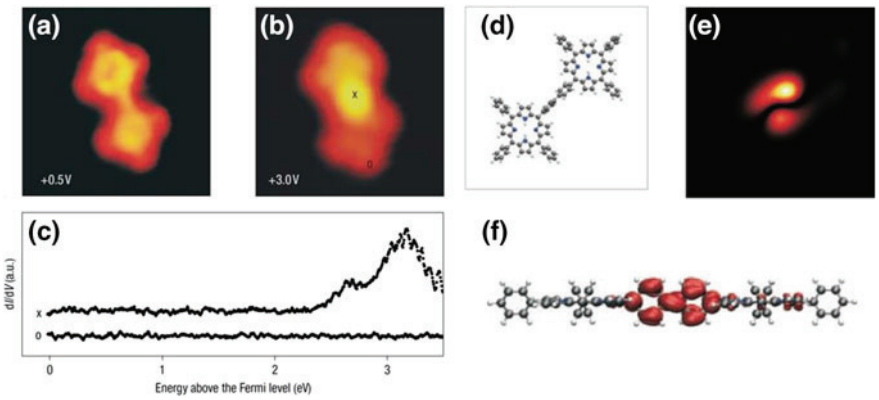


**Fig. 8** The covalent nature of intermolecular bonds. STM images (5 × 5 $nm^2$) of a TPP dimer at 0.5 V (**a**) and 3.0 V (**b**). The bright protrusion in the middle of the dimer (**b**) is a signature related to an electronic feature clearly visible in the d*I*/d*V* curve marked by a *cross* in panel (**c**). The lower d*I*/d*V* curve (marked by a *circle*) taken on top of a porphyrin leg is featureless. DFT calculations reveal the formation of a covalent bond between the two neighboring phenyl legs, with corresponding C–C bonding (*s*) and antibonding (*s**) orbitals. **d** Calculated geometric structure of the isolated dimer. **e** Calculated contribution to the local density of states due to the state at about 2.8 eV above the HOMO (at 7 Å from the porphyrin plane). **f** Side view of a three-dimensional contourplot of the orbital density of this state at a much higher density. Scanning tunneling spectroscopy (STS) was performed at 10 K with a lock-in amplifier with 20 mV peak-to-peak modulation amplitude at 640 Hz (frequency) (see caption Fig. 7 for further experimental details) [9]

options, i.e., chemical bonds as H or metal-ligand bonding and π–π stacking, can be ruled out because of the molecular structure and adsorption geometry, and additionally they could hardly explain why the nanostructure remains stable when being pulled by an STM tip.

A clear signature for the covalent nature of the intramolecular bond within the dimer is provided by spectroscopy of single molecules (by scanning tunneling spectroscopy, STS). The interconnection site within the dimer appears homogenously at low bias voltages, while it appears as a bright protrusion when imaged at +3.0 V (Fig. 8a, b). This protrusion is indeed related to an electronic broad features localized at around +3.0 V (upper STS curve in Fig. 8c) suggesting the presence of a localized orbital [9]. DFT calculations prove the local formation of a covalent C–C intermolecular bond in full agreement with the experimentally measured porphyrin cores interdistance. Specifically, the calculations revealed the formation of C–C bonding (σ) and antibonding (σ*) orbitals that give rise to the signal in the d*I*/d*V* spectra. Hence, the peak at around 3 eV is a direct fingerprint of the chemical nature of the covalent bond. It is caused by the strong interaction with the two non-occupied antibonding π orbitals associated to the two legs, resulting in an in-phase and an out-of-phase combination, which are split by 1.3 eV. The in-phase combination is responsible for the increase of the calculated local density of states precisely located in between the porphyrin cores at about 2.8 eV (Fig. 8e, f) above the highest occupied molecular orbital (HOMO). This calculated electronic feature is associated to the experimentally probed electronic feature at about 3.0 eV shown in Fig. 8 [9].

Another clear example of Ullmann dehalogenation reaction that results in polymerization on the surface was reported by the group of Rosei [19]. They deposited diiodobenzene molecular species (**1** and **2** in Fig. 9a) on Cu(110) and found at first the formation of Cu bound phenylene intermediates, i.e., not yet linked by C–C

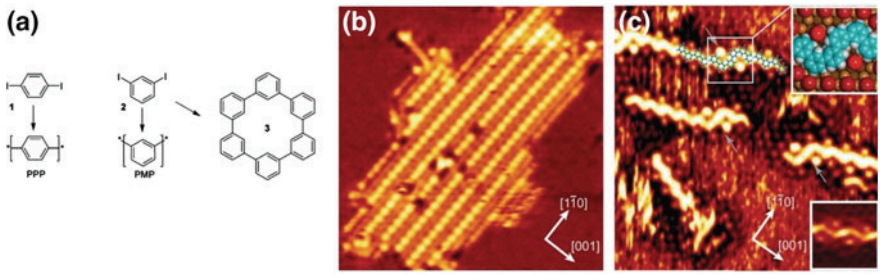


**Fig. 9** Formation of polyphenylene-based polymers by on-surface polymerization. **a** Ullmann coupling of diiodobenzene molecules. **b** STM image ($T$ = 115 K, 19 × 19 nm$^2$, $V$ = −1.93 V, I = 1.06 nA) of PPP-based olygomers. 1,3-diodobenzene (*1* in panel **a**) were dosed on Cu(110) kept at room temperature and afterwards annealed to 500 K. **c** 0.2 L of 1,3-diiodobenzene dosed onto Cu(110) held at 500 K. STM topography (11.3 × 11.3 nm$^2$, $V_s$ = −0.57 V, $I_t$ = 0.82 nA) of oligomer branches. A model of PMP is overlaid on one of the oligomers. *Top-right inset* a force field relaxed model of PMP chain in the iodine matrix on a slab of Cu corresponding to the marked region in the STM image. *Bottom right inset* a scale portion of the RT deposited surface, showing a protopolymer of molecule *2* in panel **a**. Reproduced from [19]. © 2009 Wiley-VCH Verlag GmbH & Co. KGaA, Weinheim. doi:10.1002/smll.200801943

covalent bonds when depositing molecules on the surface kept at room temperature. Heating the sample to 500 K for 5–10 min is needed to induce the formation of straight conjugated PPP olygomers (Fig. 9b). The formation of zigzag PMP wires and macrocycles as well were promoted and observed when using 1,3-diiodobenzene (Fig. 9c, kinks are ascribed to the molecular symmetry) [19].

## 5 Controlling Nanostructures by Hierarchical Growth

The results presented so far are related to the growth of simple homogeneous molecular architectures, because they are based on a one-step process. Growing complex nanostructures, e.g., more complex molecular aggregates, requires a fine and accurate control of the reaction pathway that leads to the final molecular architecture. This can be achieved splitting the reaction pathway into individual connection steps and controlling their activation sequence, thus realizing a "programmed reactivity" of the molecules that allows *selective* activation of their reactivity at different sites. A sequential growth fashion can be implemented by designing single molecular building blocks that carry different types of halogen substituents. The sample temperature can be used as an "external knob" that allows to enable or suppress specified halogen dissociations, i.e., on-surface polymerization processes can be initiated and systematically controlled via the sample temperature. The temperature needed to break C–halogen bonds is mainly defined by the halogen species and the catalytic activity of the surface. The carbon–halogen bond dissociation is activated at temperatures that decrease with the halogen atomic number. In other words, the binding energy to the carbon atom can be tuned via the type of halogen atom. Iodine dissociation from molecules can be initiated already at room temperature and completed at around 120 °C, while this temperature range goes from 100 to 250 °C for Br substituents [35, 46]. A proper choice of the surface is crucial as it has been shown that the on-surface covalent linking occurs at different temperatures for different noble metal surfaces [39], or can even be suppressed for other surfaces. Gutzler et al. [16] reported on the growth of two-dimensional covalent bound networks by using polyaromatic molecules carrying halogen substituents. They deposited these molecular species on Cu(111) and Ag(110) and indeed verified the presence of activated species already at room temperature, i.e., without the need of additional activation energy. The same procedure repeated on graphite(001) resulted in the formation of well-ordered non-covalently bound networks stabilized by halogen–hydrogen bonding. This proves the importance of the surface in promoting the carbon–halogen dissociation at room temperature and the subsequent molecular assembly.

As mentioned above, the architecture of the final structures is encoded in the single monomer building block by incorporating distinct carbon–halogen bonds that dissociate and create active sites at the halogen sites. With this purpose, a porphyrin *trans*-$Br_2I_2$TPP unit has been designed and synthesized in order to carry two different types of halogen–phenyl side groups (Fig. 10a). *Trans*-$Br_2I_2$TPP

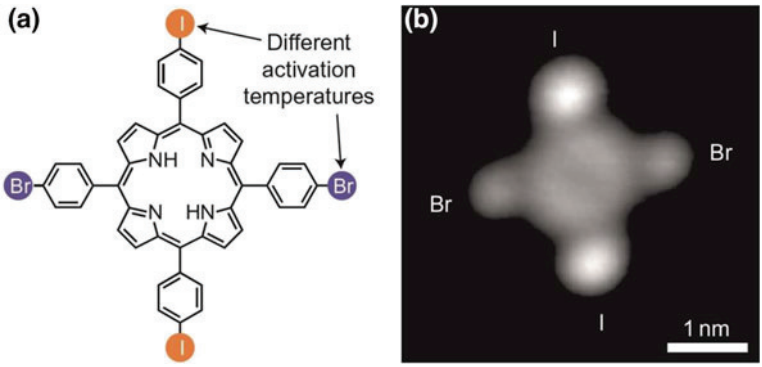


**Fig. 10** Single monomer building blocks carrying Br and I substituents for sequential activation. **a** Chemical structure of the *trans*-$Br_2I_2$TPP. Br and I chemical groups have different chemical activation temperatures. **b** STM image (0.5 V, 0.1 nA) of a single intact *trans*-$Br_2I_2$TPP on Au (111). I substituents appear brighter than Br ones because of their different chemical structure. Measurements were performed under UHV conditions with a low-temperature STM operated at a temperature of 10 K. Molecules were sublimated at 593 K onto Au(111) kept at room temperature [35]

molecules have two pairs of halogen substituents (Br and I) each of them in a *trans* configuration on opposite sides of the porphyrin unit (see Fig. 10a). This chemical structure intrinsically encodes two different growth directions. As the two substituents have a pronounced difference in terms of bond dissociation energy (the binding energy of iodine–carbon is lower than that of bromine–carbon) [35], this allows to create active sites in the molecule step-by-step. In this way, new covalent intermolecular C–C bonds are formed with geometric control (via the temperature) and consequently sequential growth of nanostructures is achieved (see growth scheme in Fig. 10a). Low-temperature STM imaging allows to resolve with sub-molecular resolution the features of intact *trans*-$Br_2I_2$TPP molecules deposited on top of Au(111): the typical four-legs structure of the porphyrin unit is recognized and substituent halogens can be chemically distinguished because of their different appearance in STM (Fig. 10b): I and Br substituents have specific apparent heights and the former look brighter independent of the bias voltage over the investigated range (−1 V, +1 V) [35]. Thus, by comparison with other porphyrin derivatives that contain either only Br or only I substituents, it is possible to assign the characteristic apparent heights to iodine and bromine substituents. This precise knowledge of the chemical composition in an STM image (Fig. 10b) is important in the next step to identify which substituents remain after a heating step and which ones are dissociated.

*Trans*-$Br_2I_2$TPP molecules have been deposited onto Au(111) while keeping the substrate at a temperature of 80 K to suppress catalytically driven iodine dissociation from the molecules that occurs at higher temperatures, thus to keep the molecules intact with all four halogen substituents [35]. Under these conditions, molecular units are preferentially found in close-packed arrangements (Fig. 11b).

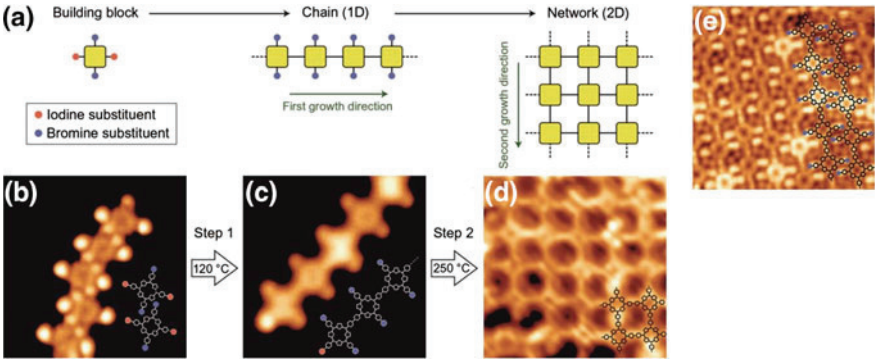


**Fig. 11** Hierarchical growth of homogeneous molecular structures. **a** Scheme of the sequential activation mechanism (from *left* to *right*). In the first activation step, I substituents are dissociated and active sites in a *trans* geometry (*first growth direction*) are created enabling the formation of linear structures (from **b** to **c**). In the second step, Br are dissociated by annealing at higher temperatures. This further step allows to create lateral active sites that enable the growth along the second growth direction, i.e., the formation of 2D networks (from **c** to **d**). STM images ($8 \times 8$ nm$^2$, **b**) of *trans*-$Br_2I_2$TPP molecules on Au(111), after heating up to 120 K (*step 1*, $8 \times 8$ nm$^2$, **c**), and after further annealing up to 250 K (*step 2*, $10 \times 10$ nm$^2$, **d**). **e** STM image ($10 \times 10$ nm$^2$) of close-packed porphyrin chains after the first activation step. Further experimental details are in caption Fig. 9 and Ref. [35]

Annealing of the sample up to room temperature induces a partial I dissociation, while annealing up to 120 °C enables an efficient polymerization across the *trans*-iodine direction (first growth direction in panel Fig. 11a) during the first step. According to the *trans*-arrangement of halogen substituents within the single monomer, linear chains of porphyrin units are grown (Fig. 11c). This is in analogy to the *trans*-$Br_2$TPP molecules (Fig. 7h) but at lower temperatures because iodine is involved here. There are two important characteristics of these intermediate products (shown in Fig. 11c): (1) These chains always have a bright loves at their end, which reflects an iodine atom (as in Fig. 10b). Hence, all newly formed bonds are located at former iodine sites, which confirms the successful selective activation in this first step. (2) The Br substituents, which appear darker than the iodines, can be clearly seen sideways at the polymer chain and are therefore still present. However, they have not been activated yet and are therefore dormant, waiting to be activated at a suitable temperature.

Furthermore, covalently linked porphyrin chains arrange themselves parallel to each other into close-packed islands (Fig. 11e). In the next growth step, Br substituents are efficiently dissociated by thermal annealing up to 250 °C enabling the polymerization process along the second growth direction (as indicated in Fig. 8a) and triggering the formation of TPP-based two-dimensional networks (Fig. 11d). This represents an elegant way to grow two-dimensional networks in a sequential manner, and it is worth to compare it with the same structure obtained by the one-step growth process (TPP-based networks in Fig. 7i, l). An analysis of the

regularity of the TPP-based networks grown following both methods suggests that the hierarchical growth allows to prepare 2D architectures with less incorrectly connected building blocks, i.e. defects, and larger spatially extent regular networks (a detailed analysis is present in [35]).

Heterogeneous molecular architectures might be grown according to a hierarchical growth scheme. Covalently linked two-component structures on metal surfaces under UHV condition have already been achieved [10], although in a one-step growth process and thus limited control. The capability to activate different reaction pathways step-by-step allows a better tuning of the growth process. While the formation of two-dimensional TPP networks could also be achieved in a one-step process (Fig. 7l), the mixture of two molecular species in addition to the selective activation mechanism leads to molecular nanostructures that cannot be formed in one step. When combining *trans*-$Br_2I_2$TPP and DBTF molecules (Fig. 12a) on a Au (111) surface the two growth steps are sequentially activated when heating the sample at 250 °C. First, iodines of *trans*-$Br_2I_2$TPP molecules are dissociated and linear porphyrin chains are created while Br-phenyl groups remain intact (Fig. 11c). Second, Br sites are dissociated and DBTF molecules form linear chains that connect to the former Br site of porphyrin building blocks (Fig. 12b). In this way a ladder-type structure is formed that could not be achieved in one step.

A detailed analysis of the covalent links at the activated phenyl groups of porphyrin building blocks (shown in Fig. 12c) reveals the high selectivity of the process: 98 % of the former I sites of *trans*-$Br_2I_2$TPP molecules are connection points for further porphyrin units as desired from the molecular design. Only 2 % of

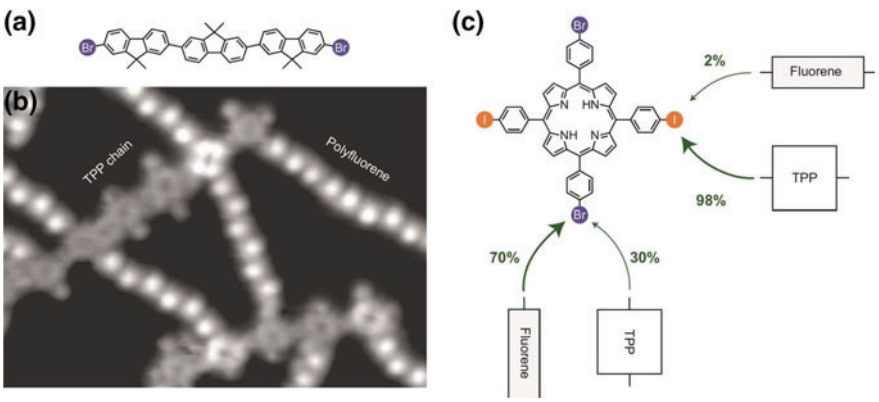


**Fig. 12** Hierarchical growth of heterogenous architectures. **a** Chemical structure of DBTF molecules. **b** STM image ($T$ = 10 K, 18 × 13 nm$^2$) of heterogenous networks based on DBTF and *trans*-$Br_2I_2$TPP on Au(111) by hierarchical growth after heating up to 250 °C. **c** Statistical analysis of porphyrin and fluorine attachment to the porphyrin *trans*-$Br_2I_2$TPP monomer at former bromine and iodine sites (number of evaluated sites: $n_I$ = 489, $n_{Br}$ = 269). Measurements were performed under UHV conditions with a low-temperature STM operated at a temperature of 10 K. A Knudsen cell was used to evaporate $Br_4$TPP molecules at 550 K and DBTF molecules at 503 K onto Au (111). The on-surface synthesis was achieved raising the sample temperature to 250 °C [35]

these sites are incorrectly used for fluorine connections. The second growth step determines a pronounced occupation of the remaining two Br sites by fluorene molecules (70 %, see Fig. 11c). The numbers are less impressive in this second case, because at the former Br sites also two porphyrin chains could be linked side to side, which represent a competition process for the planned ladder structure. This proves that the hierarchical growth leads to the formation of copolymers assisted by a remarkable degree of selectivity of the chemical species involved in the process.

## 6 Substrate-Directed Growth by On-Surface Synthesis

The on-surface synthesis consists of two processes at work: activation and diffusion of the single monomer building blocks across the surface. Elevated temperatures are required to enable these processes, but this also favors disorder into the molecular assembly and can therefore reduce the efficiency of the polymerization process. It should be noted, however, that the substrate surface is not a passive support for chemical species [16] but can play an active role in terms of activation of the molecular species in virtue of its catalytic properties [16, 41].

Any crystalline surface exhibits a certain corrugation, depending on the crystal structure and the surface orientation, which plays a crucial role for molecular diffusion. This feature can be used in order to introduce a further degree of freedom, thus improving the covalent linking and varying the final orientation of a nanostructure compared to the underlying substrate surface. By choosing properly the surface it is possible to restrict the molecular diffusion along the lowest corrugation directions and favor the formation of specific molecular architectures with a predefined orientation. For instance, the Au(110)-1 × 3 surface has been used to constrain the diffusion and subsequent polymerization of alkyl chains along its missing rows [40]. The confinement of molecular diffusion to one dimension (Fig. 13) leads to intermolecular interactions between neighboring molecules that result in the formation of linear molecular chains [40].

The effect of surface anisotropy on the growth of two-dimensional networks has been studied with an Au(100) single-crystal surface. The reconstructed surface shows a quasi-hexagonal (5 × 20) superstructure with straight rows of vertically displaced atoms [47], as shown in Fig. 14a [35]. *Trans*-$Br_2I_2$TPP molecules have been deposited on Au(100) at low temperature in order to keep all halogen–phenyl groups intact. Afterwards the sample was annealed to 120 °C. After this procedure, covalently bound porphyrin chains with a preferential orientation are found as illustrated in Fig. 14a. Hence, the surface reconstruction determines the orientation of the final nanostructure.

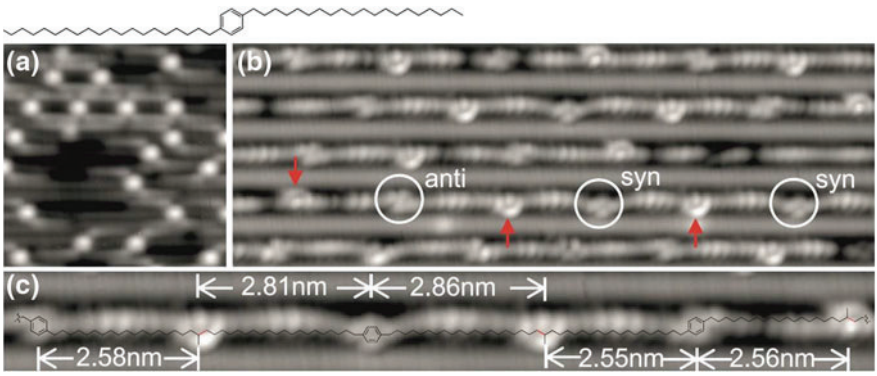


**Fig. 13** Polymerization of hydrocarbons on an anisotropic gold surfaces. **a** STM topographic image of DEB molecules (12 × 12 $nm^2$, −0.5 V, 0.5 nA) on Au(110)-1 × 2 at 300 K. **b** STM topographic image (17.5 × 6 $nm^2$, −1 V, 2 nA) polymerized DEB chains located in the missing rows of Au(110)-1 × 3 after heating at 420 K for 10 h. *Circles* denote the phenylene groups; *arrows* denote the methyl side groups. **c** A section of DEB polymer chain and superimposed the molecular structure (14.4 × 1.6 $nm^2$, −1 V, 2 nA). The newly formed C–C bonds are shown in *red*. From [40]. Reprinted with permission from American Association for the Advancement of Science

An analysis of the chains angular distribution reveals a preferred angle at 51° between chains and atomic rows (Fig. 14b). This finding can be easily rationalized by geometric arguments since all porphyrin units are adsorbed on equivalent sites (Fig. 14c), thus reducing the total energy by this particular angle [35]. This is in contrast to the rather flat Au(111) surface where the angular distribution of chains is less defined (Fig. 7 and Ref. [1]) and underlines the importance of the surface corrugation. After heating to 250 °C (the second activation step), formation of rectangular networks is again found (Fig. 14d) with a clear orientation off the Au (100) atomic rows orientation [35]. Small networks reveal deviations from the rectangular shape (angle $\beta = 101 \pm 3°$ instead of 90°) as shown in Fig. 14d. This effect is most likely ascribed to the reduced relative contribution of intermolecular bond energy compared to the interaction of the molecular assembly with the surface [35] for small networks. Furthermore, a larger average size of networks is achieved as compared to the Au(111) surface [35], which can directly be assigned to the surface anisotropy. The corrugation rows lead to a parallel arrangement of the intermediate products (as illustrated in Fig. 14a) that results in a sort of zipping mechanism for the two-dimensional linking in the second step: If the first link between two chains is established, all other porphyrin units are in a perfect arrangement with respect to each other and a rather efficient linking of long chain segments can occur. As a consequence, the final nanostructures are larger for hierarchical growth on a corrugated surface than in a single-step process.

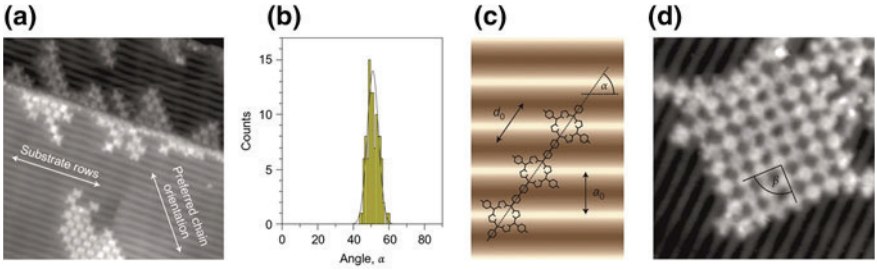


**Fig. 14** Substrate-directed growth of networks. **a** STM image (42 × 42 nm$^2$) of *trans*-$Br_2I_2$TPP chains grown on Au(100) after the first activation process. **b** Angular distribution for chains shown in panel **a**. **c** Adsorption geometry scheme of polymeric chain on Au(100) surface with an angle of 55° for equivalent adsorption sites for all porphyrins ($a_0$ = 1.44 nm and $d_0$ = 1.76 nm). **d** STM image (20 × 20 nm$^2$) of an approximately squared covalently linked molecular network after the second activation process. Measurements were performed under UHV conditions with a low-temperature scanning tunneling microscope (STM) operated at a temperature of 10 K. A Knudsen cell was used to evaporate $Br_4$TPP molecules at 550 K onto Au(100). The first and second activation steps were induced by heating to 120 and 250 °C, respectively [35]

## 7 Summary

The growth of molecular nanostructures on surfaces via Ullmann coupling can be controlled by both the chemical structure of the initial building blocks, which is precisely reflected in the final products, as well as the surface underneath, in particular the presence of defects, step edges, and adatoms. Diffusion of the activated monomers and intermediate oligomers is another key issue since it defines the rate of polymerization and the possibility of substrate-directed growth that allows improved linking reactions. Various molecules have been used in the last years and it turns out that on-surface polymerization represents a very feasible method to create stable covalent 1D and 2D polymers on a surface and to image them by scanning probe microscopy in real space as successfully demonstrated in many cases. The covalent nature of the newly created bond is not only evident from the real space distances and orientations, but could additionally be proven by spectroscopic detection of characteristic electronic states. When using different halogen substituents, a hierarchical growth scheme could be realized since selective and sequential activation of the different substituents results in a programmed reactivity of the molecules. Based on the gathered mechanistic insight and with the ability to direct reactivity by designing proper monomer building blocks as well as using the surface as a template, 1D and 2D polymers of increasing structural and compositional complexity will emerge. Besides this continued exploration of on-surface polymerization as a new method for generating defined nanostructures, their resulting properties and functions will become increasingly important in the future.

## References


1. Joachim, C., Gimzewski, J.K., Aviram, A.: Electronics using hybrid-molecular and mono-molecular devices. Nature **408**, 541–548 (2000)
2. Heath, J.R., Ratner, M.A.: Molecular Electronics. Phys. Today **56**, 43–49 (2003)
3. Wintterlin, J., Bocquet, M.-L.: Graphene on metal surfaces. Surf. Sci. **603**, 1841–1852 (2009)
4. Nagashima, A., Tejima, N., Gamou, Y., Kawai, T., Oshima, C.: Electronic dispersion relations of monolayer hexagonal boron nitride formed on the Ni(111) surface. Phys. Rev. B **51**, 4606–4613 (1995)
5. Rabe, J.P., Buchholz, S.: Commensurability and mobility in two-dimensional molecular patterns on graphite. Science **253**, 424–427 (1991)
6. Yokoyama, T., Yokoyama, S., Kamikado, T., Okuno, Y., Mashiko, S.: Selective assembly on a surface of supramolecular aggregates with controlled size and shape. Nature **413**, 619–621 (2001)
7. Theobald, J.A., Oxtoby, N.S., Phillips, M.A., Champness, N.R., Beton, P.H.: Controlling molecular deposition and layer structure with supramolecular surface assemblies. Nature **424**, 1029–1031 (2003)
8. Schlickum, U., Decker, R., Klappenberger, F., Zoppellaro, G., Klyatskaya, S., Ruben, M., Silanes, I., Arnau, A., Brune, H., Barth, J.V.: Metal-organic honeycomb nanomeshes with tunable cavity size. Nano Lett. **7**, 3813–3817 (2007)
9. Grill, L., Dyer, M., Lafferentz, L., Persson, M., Peters, M.V., Hecht, S.: Nano-architectures by covalent assembly of molecular building blocks. Nature Nanotech. **2**, 687–691 (2007)
10. Weigelt, S., Busse, C., Bombis, C., Knudsen, M.M., Gothelf, K.V., Strunskus, T., Wöll, C., Dahlbom, M., Hammer, B., Lægsgaard, E., Besenbacher, F., Linderoth, T.R.: Covalent interlinking of an aldehyde and an amine on an Au(111) surface in ultrahigh vacuum. Angew. Chem. Int. Ed. **46**, 9227–9230 (2007)
11. Champness, N.R.: Surface chemistry: building with molecules. Nature Nanotech. **2**, 671–672 (2007)
12. Matena, M., Riehm, T., Stöhr, M., Jung, T.A., Gade, L.H.: Transforming surface coordination polymers into covalent surface polymers: linked polycondensed aromatics through oligomerization of N-heterocyclic carbene intermediates. Angew. Chem. Int. Ed. **47**, 2414–2417 (2008)
13. Veld M.I., Iavicoli P., Haq S., Amabilino D.B., Raval R.: Unique intermolecular reaction of simple porphyrins at a metal surface gives covalent nanostructures. Chem. Commun. 1536–1538 (2008)
14. Zwaneveld, N.A.A., Pawlak, R., Abel, M., Catalin, D., Gigmes, D., Bertin, D., Porte, L.: Organized formation of 2D extended covalent organic frameworks at surfaces. J. Am. Chem. Soc. **130**, 6678–6679 (2008)
15. Gourdon, A.: On-surface covalent coupling in ultrahigh vacuum. Angew. Chem. Int. Ed. **47**, 6950–6953 (2008)
16. Gutzler, R., Walch, H., Eder, G., Kloft, S., Heckl, W.M., Lackinger, M.: Surface mediated synthesis of 2D covalent organic frameworks: 1,3,5-tris(4-bromophenyl)benzene on graphite (001), Cu(111), and Ag(110). Chem. Commun. 4456–4458 (2009)
17. Perepichka, D.F., Rosei, F.: Extending polymer conjugation into the second dimension. Science **323**, 216–217 (2009)
18. Sakamoto, J., Van Heijst, J., Lukin, O., Schlüter, A.D.: Two-dimensional polymers: Just a dream of synthetic chemists? Angew. Chem. Int. Ed. **48**, 1030–1069 (2009)
19. Lipton-Duffin, J.A., Ivasenko, O., Perepichka, D.F., Rosei, F.: Synthesis of polyphenylene molecular wires by surface-confined polymerization. Small **5**, 592–597 (2009)
20. Bartels, L.: Tailoring molecular layers at metal surfaces. Nature Chem. **2**, 87–95 (2010)
21. Lipton-Duffin, J.A., Miwa, J.A., Kondratenko, M., Cicoira, F., Sumpter, B.G., Meunier, V., Perepichka, D.F., Rosei, F.: Step-by-step growth of epitaxially aligned polythiophene by surface-confined reaction. Proc. Natl. Acad. Sci. **107**, 11200–11204 (2010)

22. Lackinger, M., Heckl, W.M.: A STM perspective on covalent intermolecular coupling reactions on surfaces. J. Phys. D Appl. Phys. **44**, 464011 (2011)
23. Mendez, J., Lopez, M.F., Martin-Gago, J.A.: On-surface synthesis of cyclic organic molecules. Chem. Sov. Rev. **40**, 4578–4590 (2011)
24. Ouchi, M., Badi, N., Lutz, J.-F., Sawamoto, M.: Single-chain technology using discrete synthetic macromolecules. Nature Chem. **3**, 917–924 (2011)
25. Palma, C.-A., Samorì, P.: Blueprinting macromolecular electronics. Nature Chem. **3**, 431–436 (2011)
26. Colson, J.W., Dichtel, W.R.: Rationally synthesized two-dimensional polymers. Nat. Chem. **5** (6), 453–465 (2013)
27. El Garah, M., MacLeod, J.M., Rosei, F.: Covalently bonded networks through surface-confined polymerization. Surf. Sci. **613**, 6–14 (2013)
28. Grill, L.: Functionalized molecules studied by STM: motion, switching and reactivity. J. Phys.: Condens. Matter **20**, 053001 (2008)
29. Nitzan, A., Ratner, M.A.: Electron transport in molecular wire junctions. Science **300**, 1384–1389 (2003)
30. Lafferentz, L., Ample, F., Yu, H., Hecht, S., Joachim, C., Grill, L.: Conductance of a single conjugated polymer as a continuous function of its length. Science **323**, 1193–1197 (2009)
31. Koch, M., Ample, F., Joachim, C., Grill, L.: Voltage-dependent conductance of a single graphene nanoribbon. Nature Nanotech. **7**, 713–717 (2012)
32. Ullmann, F., Bielecki, J.: Ueber synthesen in der Biphenylreihe. Chem. Ber. **34**, 2174 (1901)
33. Barth, J.V., Costantini, G., Kern, K.: Engineering atomic and molecular nanostructures at surfaces. Nature **437**, 671–679 (2005)
34. De Greef, T.F.A., Smulders, M.M.J., Wollfs, M., Schenning, A.P.H.J., Sijbesma, R.P., Meijer, E.W.: Supramolecular polymerization. Chem. Rev. **109**, 5687–5754 (2009)
35. Lafferentz, L., Eberhardt, V., Dri, C., Africh, C., Comelli, G., Esch, F., Hecht, S., Grill, L.: Controlling on-surface polymerization by hierarchical and substrate-directed growth. Nature Chem. **4**, 215–220 (2012)
36. Hla, S.-W., Bartels, L., Meyer, G., Rieder, K.H.: Inducing all steps of a chemical reaction with the scanning tunneling microscope tip: towards single molecule engineering. Phys. Rev. Lett. **85**(13), 2777–2780 (2000)
37. Kittelmann, M., Rahe, P., Nimmrich, M., Hauke, C.M., Gourdon, A., Kühnle, A.: On-surface covalent linking of organic building blocks on a bulk insulator. ACS Nano **5**, 8420–8425 (2011)
38. Hassan, J., Sévignon, M., Gozzi, C., Schulz, E., Lemaire, M.: Aryl-aryl bond formation one century after the discovery of the Ullmann reaction. Chem. Rev. **102**, 1359–1470 (2002)
39. Bieri, M., Nguyen, M.-T., Gröning, O., Cai, J., Treier, M., Aït-Mansour, K., Ruffieux, P., Pignedoli, C.A., Passerone, D., Kastler, M., Müllen, K., Fasel, R.: Two-dimensional polymer formation on surfaces: insight into the roles of precursor mobility and reactivity. J. Am. Chem. Soc. **132**, 16669–16676 (2010)
40. Zhong, D., Franke, J.H., Podiyanachari, S.K., Blömker, T., Zhang, H., Kehr, G., Erker, G., Fuchs, H., Chi, L.: Linear alkane polymerization on a gold surface. Science **334**, 213–216 (2011)
41. Saywell, A., Schwarz, J., Hecht, S., Grill, L.: Polymerization on stepped surfaces: alignment of polymers and identification of catalytic sites. Angew. Chem. Int. Ed. **51**, 5096–5100 (2012)
42. Wang, W., Shi, X., Wang, S., Van Hove, M.A., Lin, N.: Single-molecule resolution of an organometallic intermediate in a surface-supported Ullmann coupling reaction. J. Am. Chem. Soc. **133**, 13264–13267 (2011)
43. Koch, M., Gille, M., Viertel, A., Hecht, S., Grill, L.: Substrate-controlled linking of molecular building blocks: Au(111) vs. Cu(111). Surf. Sci. **627**, 70–74 (2014)
44. Villagomez, C.J., Sasaki, T., Tour, J.M., Grill, L.: Bottom-up assembly of molecular wagons on a surface. J. Am. Chem. Soc. **132**, 16848 (2010)
45. Rowan, S.J., Cantrill, S.J., Cousins, G.R., Stoddart, J.K., Sanders, J.F.: Dynamic covalent chemistry. Angew. Chem. Int. Ed. **41**, 898–952 (2002)

46. Krasnikov, S.A., Doyle, C.M., Sergeeva, N.N., Preobrajenski, A.B., Vinogradov, N.A., Sergeeva, Y.N., Zakharov, A.A., Senge, M.O., Cafolla, A.A.: Formation of extended covalently bonded Ni porphyrin networks on the Au(111) surface. Nano Res. **4**, 376–384 (2011)
47. Havu, P., Blum, V., Havu, V., Rinke, P., Scheffler, M.: Large-scale surface reconstruction energetics of Pt(100) and Au(100) by all-electron density functional theory. Phys. Rev. B **82**, 161418 (2010)